© Mehtapress 2013
J.Phy.Ast.

Print-ISSN: 2320-6756
Online-ISSN: 2320-6764

Journal of
Physics & Astronomy

WWW.MEHTAPRESS.COM

Full Paper

K.Ghaderi*, T.Rostami, M.H.Baghadam

Department of Science and Engineering, Islamic Azad University, Marivan Branch, Marivan, (IRAN)
E-mail: K.Ghaderi.60@gmail.com

Received: June 24, 2013
Accepted: August 30, 2013

***Corresponding author's Name & Address**

K.Ghaderi
Department of Science and Engineering, Islamic Azad University, Marivan Branch, Marivan, (IRAN)
E-mail: K.Ghaderi.60@gmail.com

New tool to derive the orbital parameters and radial velocity curve analysis of the spectroscopic binary systems

Abstract

Using measured radial velocity data of five double-lined spectroscopic binary systems 66 And, HR 6979, HR 9059, Par 1802 and QX Car (HD 86118), we find corresponding orbital and spectroscopic elements via a Probabilistic Neural Network (PNN). Our numerical results are in good agreement with those obtained by others using more traditional methods.

Key Words

Stars: binaries: eclipsing; Stars: binaries: spectroscopic.

INTRODUCTION

Analysis of both light and radial velocity (hereafter V_R) curves of binary systems helps us to determine the masses and radii of individual stars. There are different methods to determine the orbit of a spectroscopic binary from its V_R curve. Lehmann-Filhés[13] introduced a geometrical method to determine the orbital elements from the geometrical properties of the V_R curve, especially its maxima and minima. The method of Lehmann-Filhés[13] has been found to be very useful and little, if any, longer than other methods, providing a planimeter is used. This method also gives, for improving the final solution of the orbit, the differential corrections to the preliminary elements using the form of the equations of condition obtained by the method of least squares. Russell[18] suggested an analytical method to develop the observed V_R into a trigonometric series (Fourier series) and the elements are found by comparing this series with the corresponding analytical expression (Fourier series) for the velocity. In this method the time consumed is considerably longer than the method of Lehmann-Filhés[13] and when the eccentricity is much greater than 0.4, it becomes laborious. King[12] proposes a graphical method which enables one to use the whole course of the velocity curve in finding the preliminary elements, and is applicable to orbits of any eccentricity. This method depends on the velocities at equal intervals of time, as read from a freehand curve drawn to represent the observations. Schlesinger[20] presented the method of least squares which differentially corrects the preliminary orbital elements by the help of the equations of condition. The method of Schlesinger is suitable for all orbits except those with very small eccentricities. It has greater accuracy and also enables one to vary all of the unknown parameters simultaneously instead of one or two of them at a time. Russell[19] developed a quick method analogous to the graphical method of King[12] that is equally applicable to orbits of all eccentricities. It has the advantage that a single diagram takes the place of the numerous protractors which must be constructed for each separate value of the eccentricity. The graphical processes in Kings method, which demands the exact drawing of lines and measurement of angles, will consume more time than the quick method of Russell[19]. Sterne[26] described two forms of least square solutions both of which allow the differential corrections to a set of preliminary elements obtained by any direct method like the methods of Russell[18,19]. The first form is a modification of Schlesingers method[20], in which the date of periastron passage is replaced by the date at which the mean longitude is zero. The first form is suitable for all orbits except those with very small eccentricities. The second form is particularly suitable for orbits having very small eccentricities. Singh[21] introduced an approach similar to the method of Russell[18] for expanding the V_R as a trigonometric series. This method gives a standard set of velocity curves for a set of eccentricity and longitude of periastron values that can be used for the determination of preliminary elements preparatory to a least square correction. Karami & Teimoorinia[9] introduced a new non-linear least squares velocity curve analysis technique for spectroscopic binary stars. Their method was applicable to orbits of all eccentricities and inclination angles and the time consumed was considerably less than the method of Lehmann-Filhés[13]. They showed the validity of their new method to a wide range of different types of binary. See Karami & Mohebi[7,8,11] and Karami et al.[10].

However, a large number of practical methods have been proposed. But it is not useful to discuss their relative advantages: the method which gives the best results in one case may well be unsuitable in another. For instance, for near circular orbits when the eccentricity is small, the V_R curve approaches in form the simple sine curve and graphical methods cease to be of value. It is then that analytical methods become useful. See Curtis[4], Plummer[17] and Sterne[26]. Lucy and Sweeney[14] suggested that because of observational errors, most of the spectroscopic binaries with eccentricities close to zero should really be assigned circular orbits. Their argument is based on purely statistical considerations, regardless of orbital period, and has been subsequently challenged by other authors. For instance, Skuljan et al.[22] emphasize that modern observations do support the idea of Lucy and Sweeney[14], at least for the shortest-period binaries (e.g. with period less than about 10 days for late-type dwarfs). However, the situation at longer periods is not clear and the single-lined spectroscopic binary star æ TrA is one such example. They point out that the orbit of æ TrA was proved to be a definite ellipse, although with an extremely small eccentricity of 0.01442. There is always the possibility that a third low mass, unseen component could have perturbed the orbit of æ TrA to non-circularity. Concerning the evolution of low mass members of close binary systems see Han et al.[6] and Yakut and Eggleton[27].

Artificial Neural Networks have become a popular tool in almost every field of science. In recent years, ANNs have been widely used in astronomy for applications such as star/galaxy discrimination, morphological classification of galaxies, and spectral classification of stars (see Bazarghan et al.[2] and references therein). Following Bazarghan et al.[2], we employ Probabilistic Neural Networks (PNNs). This network has been investigated in ample details by Bazarghan et al.[2].

Probabilistic Neural Network (PNN) is a new tool to derive the orbital parameters of the spectroscopic binary stars. In this method the time consumed is considerably less than the method of Lehmann-Filhés and even less than the non-linear regression method proposed by Karami & Teimoorinia[9]. In the present paper we use a Probabilistic Neural Network (PNN) to find the optimum match to the four parameters of the V_R curves of the five double-lined spectroscopic binary systems: 66 And, HR 6979, HR 9059, Par 1802 and QX Car (HD 86118). Our aim is to show the validity of our new method to a wide range of different types of binary.

The star 66 And is a double-lined spectroscopic binary and consists of primary and secondary components and the minimum masses from orbit are about $0.45M_{\odot}$, or three times smaller than expected for the spectral type. The spectral type is F4 dwarf and F5 dwarf for the primary and the secondary star, respectively, and the orbital period is P = 10.989861 days[5]. HR 6979 is a double-lined spectroscopic binary and consists of primary and secondary components and unlike 66 And, the minimum masses for the components of HR 6979 are large, 1.8 and $1.7M_{\odot}$, suggesting that the components might eclipse. Both components of HR 6979 are Am stars that are still on the main sequence and the orbital period is P = 14.364577 days[5]. HR 9059 is a double-lined spectroscopic binary and consists of primary and secondary components and like HR 6979, the minimum masses of HR 9059 are rather large, in this case nearly $1.6M_{\odot}$, and so eclipses are a possibility. The components of HR 9059 have spectral classes of F5 and the orbital period is P = 12.156168 days[5]. Par 1802 is a pre-main-sequence (PMS), low-mass, double-lined, spectroscopic, eclipsing binary in the Orion star-forming region. Par 1802 is composed of two equal-mass (0.39 ± 0.03, $0.40 \pm 0.03\ M_{\odot}$) stars in a circular, P = 4.673845 day orbit and the spectral type is M2[3]. QX Car (HD 86118) is a double-lined eclipsing binary system and consists of primary and secondary components. The two components appear to be of nearly equal spectral type and luminosity, the primary having slightly stronger lines than the secondary and the spectral type is B2V and the orbital period is P = 4.4779741 days[1].

This paper is organized as follows. In Sect. 2, we introduce a Probabilistic Neural Network (PNN) to estimate the four parameters of the V_R curve. In Sect. 3, the numerical results are reported, while the conclusions are given in Sect. 4.

V_R CURVE PARAMETERS ESTIMATION BY THE PROBABILISTIC NEURAL NETWORKS (PNN)

Following Smart[23], the V_R of a star in a binary system is defined as follows

$$V_R = \gamma + K[\cos(\theta + \omega) + e\cos\omega] \quad (1)$$

where γ is the V_R of the center of mass of system with respect to the sun. Also K is the amplitude of the V_R of the star with respect to the center of mass of the binary. Furthermore θ, ω and e are the angular polar coordinate (true anomaly), the longitude of periastron and the eccentricity, respectively.

Here we apply the PNN method to estimate the four orbital parameters, γ, K, e and ω of the V_R curve in Eq. (1). In this work, for the identification of the observational V_R curves, the input vector is the fitted V_R curve of a star. The PNN is first trained to classify V_R curves corresponding to all the possible combinations of γ, K, e and ω. For this one can synthetically generate V_R curves given by Eq. (1) for each combination of the parameters:

- $-100 \le \gamma \le 100$ in steps of 1;
- $1 \le K \le 300$ in steps of 1;
- $0 \le e \le 1$ in steps of 0.001;
- $0 \le \omega \le 360°$ in steps of 5;

This gives a very big set of k pattern groups, where k denotes the number of different V_R classes, one class for each combination of γ, K, e and ω. Since this very big number of different V_R classes leads to some computational limitations, hence one can first start with the big step sizes. Note that from Petrie[16], one can guess γ, K and e from a V_R curve. This enable one to limit the range of parameters around their initial guesses. When the preliminary orbit was derived after several stages, then one can use the above small step sizes to obtain the final orbit. The PNN has four layers including input, pattern, summation, and output layers, respectively (see Figure 5 in Bazarghan et al.[2]). When an input vector is presented, the pattern layer computes distances from the input vector to the training input vectors and produces a vector whose elements indicate how close the input is to a training input. The summation layer sums these contributions for each class of inputs to produce as its net output a vector of probabilities. Finally, a competitive transfer function on the output layer picks the maximum of these probabilities, and produces a 1 for that class and a 0 for the other classes[24,25]. Thus, the PNN classifies the input vector into a specific k class labeled by the four parameters γ, K, e and ω because that class has the maximum probability of being correct.

NUMERICAL RESULTS

Here, we use the PNN to derive the orbital elements for the five different double-lined spectroscopic systems 66 And, HR 6979, HR 9059, Par 1802 and QX Car (HD 86118). Using measured V_R data of the two components of these systems obtained by Fekel et al.[5] for 66 And, HR 6979 and HR 9059, Cargile et al.[3] for Par 1802 and Andersen et al.[1] for QX Car(HD 86118), the fitted velocity curves are plotted in terms of the phase in Figures 1 to 5.

The orbital parameters obtaining from the PNN for 66 And, HR 6979, HR 9059, Par 1802 and QX Car (HD 86118) are tabulated in TABLES 1, 3, 5, 7 and 9, respectively. Tables show that the results are in good accordance with the those obtained by Fekel et al.[5] for 66 And, HR 6979 and HR 9059, Cargile et al.[3] for Par 1802 and Andersen et al.[1] for QX Car(HD 86118).

Note that the errors of the orbital parameters in TABLES 1, 3, 5, 7 and 9 are the same selected steps for generating V_R curves, i.e. $\Delta\gamma = 1$, $\Delta K = 1$, $\Delta e = 0.001$ and $\Delta\omega = 5$. These are close to the observational errors reported in the literature. Regarding the estimated errors, following Specht[25], the error of the decision boundaries depends on the accuracy with which the underlying Probability Density Functions (PDFs) are estimated. Parzen[15] proved that the expected error gets smaller as the estimate is based on a large data set. This definition of consistency is particularly important since it means that the true distribution will be approached in a smooth manner. Specht[25] showed that a very large value of the smoothing parameter would cause the estimated errors to be Gaussian regardless of the true underlying distribution and the misclassification rate is stable and does not change dramatically with small changes in the smoothing parameter.

The combined spectroscopic elements including $m_p \sin^3 i$, $m_s \sin^3 i$, $(m_p + m_s)\sin^3 i$, $(a_p + a_s)\sin i$ and $\frac{m_s}{m_p}$ are calculated by substituting the estimated parameters K, e and ω into Eqs. (3), (15) and (16) in Karami and Teimoorinia[9]. The results obtained for the five systems are tabulated in TABLES 2, 4, 6, 8 and 10 show that our results are in good agreement with the those obtained Fekel et al.[5] for 66 And, HR 6979 and HR 9059, Cargile et al.[3] for Par 1802 and Andersen et al.[1] for QX Car(HD 86118), respectively. Here the errors of the combined spectroscopic elements in TABLES 2, 4, 6, 8 and 10 are obtained by the help of orbital parameters errors. See again Eqs. (3), (15) and (16) in Karami and Teimoorinia[9].

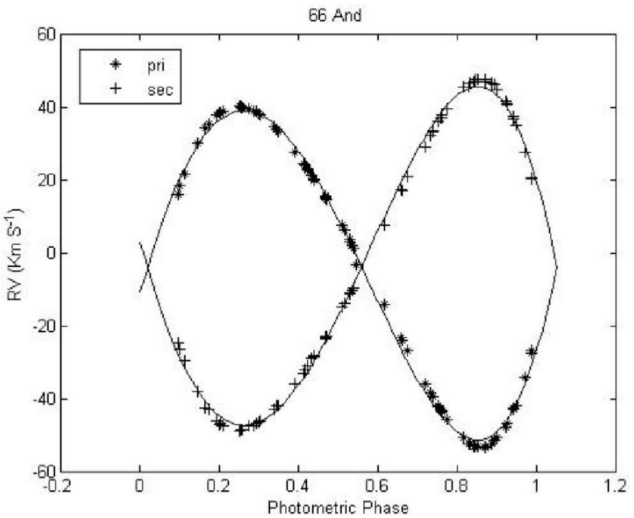

Figure 1 : Radial velocities of the primary and secondary components of 66 And plotted against the phase. The observational data have been measured by Fekel et al.[5].

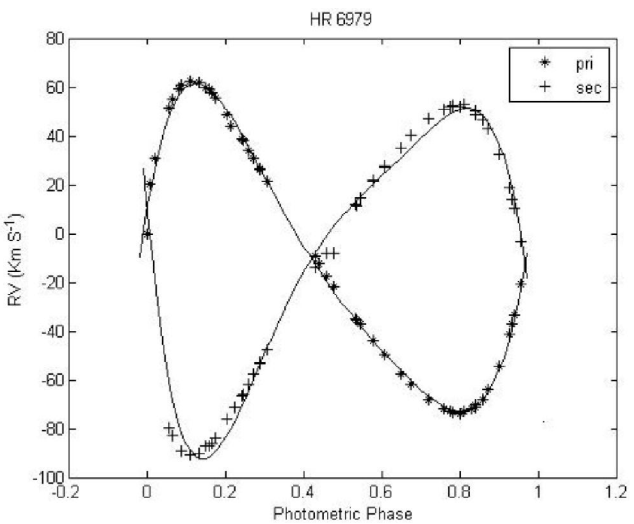

Figure 2 : Radial velocities of the primary and secondary components of HR 6979 plotted against the phase. The observational data have been measured by Fekel et al.[5].

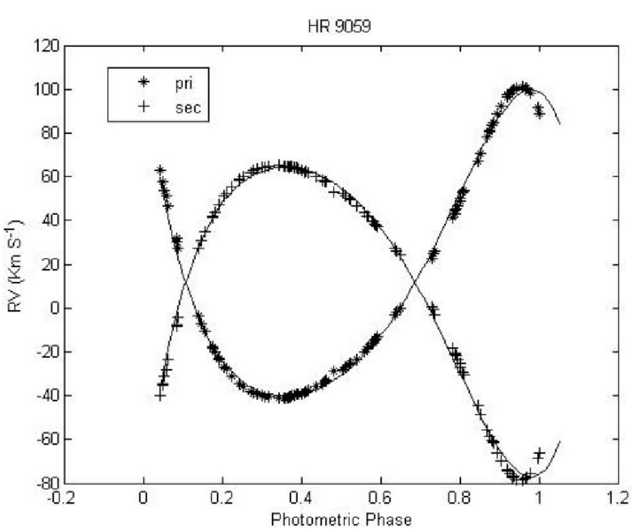

Figure 3 : Radial velocities of the primary and secondary components of HR 9059 plotted against the phase. The observational data have been measured by Fekel et al.[5].

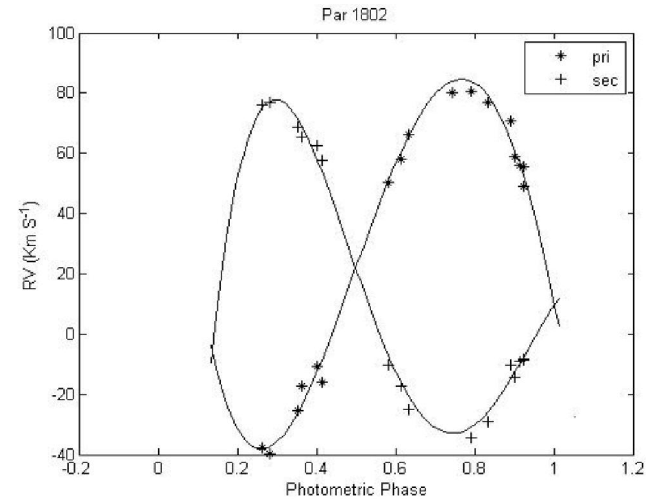

Figure 4 : Radial velocities of the primary and secondary components of Par 1802 plotted against the phase. The observational data have been measured by Cargile et al.[3].

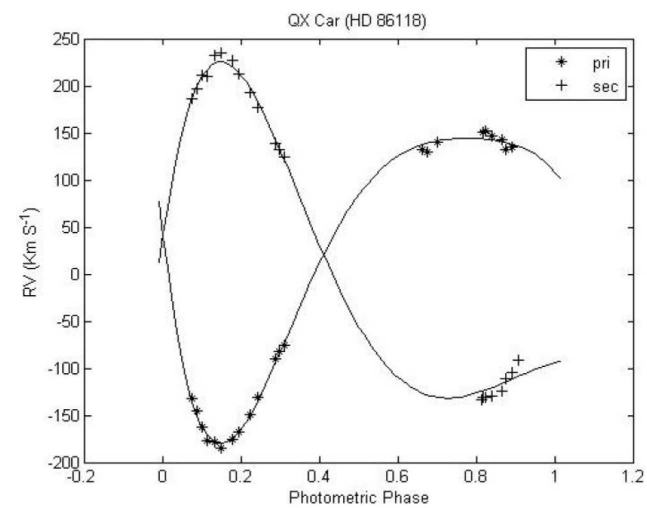

Figure 5 : Radial velocities of the primary and secondary components of QX Car (HD 86118) plotted against the phase. The observational data have been measured by Andersen et al.[1].

TABLE 1 : Orbital parameters of 66 And

	This Paper	Fekel et al.[5]
γ(km / s)	-4 ± 1	-3.705 ± 0.019
K_p (km / s)	47 ± 1	46.719 ± 0.034
K_s (km /s)	48 ± 1	48.083 ± 0.038
e	0.193 ± 0.001	0.19236 ± 0.00057
ω(°)	255 ± 5	250.55 ± 0.18

TABLE 2 : Combined spectroscopic elements of 66 And

Parameter	This Paper	Fekel et al.[5]
$m_p \sin^3 i / M$	0.4659 ± 0.0296	0.4661 ± 0.0008
$m_s \sin^3 i / M$	0.4562 ± 0.0292	0.4529 ± 0.0007
$(m_p + m_s) \sin^3 i / M$	0.9222 ± 0.0588	—
$a_p \sin i / 10^6$ km	6.9692 ± 0.1497	6.9283 ± 0.0051
$a_s \sin i / 10^6$ km	7.1174 ± 0.1497	7.1306 ± 0.0056
$(a_p + a_s) \sin i / 10^6$ km	14.0866 ± 0.2994	—
m_s / m_p	0.9792 ± 0.0416	—

TABLE 3 : Orbital parameters of HR 6979

	This Paper	Fekel et al.[5]
γ(km / s)	-12 ± 1	-12.252 ± 0.026
K_p (km / s)	68 ± 1	68.006 ± 0.043
K_s (km / s)	72 ± 1	71.790 ± 0.060
E	0.304 ± 0.001	0.30517 ± 0.00049
ω(°)	285 ± 5	289.14 ± 0.11

TABLE 4 : Combined spectroscopic elements of HR 6979

Parameter	This Paper	Fekel et al.[5]
$m_p \sin^3 i$ / M	1.8159 ± 0.0789	1.8075 ± 0.0031
$m_s \sin^3 i$ / M	1.7150 ± 0.0759	1.7122 ± 0.0025
$(m_s + m_s) \sin^3 i$ / M	3.5310 ± 0.1549	—
$a_p \sin i$ / 10^6 km	12.7961 ± 0.1925	12.792 ± 0.008
$a_s \sin I$ / 10^6 km	13.5489 ± 0.1927	13.504 ± 0.012
$(a_p + a_s) \sin i$ / 10^6 km	26.3450 ± 0.3852	—
m_s / m_p	0.9444 ± 0.0276	—

TABLE 5 : Orbital parameters of HR 9059

	This Paper	Fekel et al.[5]
γ(km / s)	12 ± 1	11.744 ± 0.014
K_p (km / s)	71 ± 1	71.117 ± 0.027
K_s (km / s)	72 ± 1	71.905 ± 0.026
e	0.312 ± 0.001	0.31167 ± 0.00026
ω(°)	30 ± 5	34.453 ± 0.052

TABLE 6 : Combined spectroscopic elements of HR 9059

Parameter	This Paper	Fekel et al.[5]
$m_p \sin^3 i$ / M	1.5903 ± 0.0682	1.5930 ± 0.0013
$m_s \sin^3 i$ / M	1.5682 ± 0.0676	1.5755 ± 0.0013
$(m_p + m_s) \sin^3 i$ / M	3.1585 ± 0.1358	—
$a_p \sin I$ / 10^6 km	11.2759 ± 0.1627	11.296 ± 0.004
$a_s \sin I$ / 10^6 km	11.4347 ± 0.1628	11.421 ± 0.004
$(a_p + a_s) \sin i$ / 10^6 km	22.7106 ± 0.3255	—
m_s / m_p	0.9861 ± 0.0283	—

TABLE 7 : Orbital parameters of Par 1802

	This Paper	Cargile et al.[3]
γ(km / s)	22 ± 1	21.9 ± 0.6
K_p (km / s)	60 ± 1	60.0 ± 1.1
K_s (km / s)	58 ± 1	58.1 ± 1.1
e	0.020 ± 0.001	0.02 ± 0.02
ω(°)	50 ± 5	54.3 ± 39.0

TABLE 8 : Combined spectroscopic elements of Par 1802

Parameter	This Paper	Cargile et al.[3]
$m_p \sin^3 i$ / M	0.3908 ± 0.0200	0.40 ± 0.03
$m_s \sin^3 i$ / M	0.4043 ± 0.0205	0.40 ± 0.03
$(m_p + m_s) \sin^3 i$ / M	0.7951 ± 0.0405	—
$a_p \sin i$ (AU)	0.0258 ± 0.0005	—
$a_s \sin i$ (AU)	0.0249 ± 0.0005	—
$(a_p + a_s) \sin i$ (AU)	0.0507 ± 0.0010	0.0507 ± 0.0004
m_s / m_p	0.9667 ± 0.0328	0.97 ± 0.03

TABLE 9 : Orbital parameters of QX Car(HD 86118)

	This Paper	Andersen et al.[1]
γ(km / s)	17 ± 1	17.0 ± 2.0
K_p (km / s)	167 ± 1	167.0 ± 1.1
K_s (km / s)	183 ± 1	182.5 ± 1.0
e	0.277 ± 0.001	0.278 (fixed)
ω(°)	125 ± 5	123.6 (fixed)

TABLE 10 : Combined spectroscopic elements of QX Car(HD 86118)

Parameter	This Paper	Andersen et al.[1]
$m_p \sin^3 i$ / M	9.2268 ± 0.1642	9.19 ± 0.12
$m_s \sin^3 i$ / M	8.4201 ± 0.1542	8.41 ± 0.12
$(m_p + m_s) \sin^3 i$ / M	17.6468 ± 0.3184	—
$a_p \sin I$ / R	14.1967 ± 0.0893	—
$a_s \sin i$ / R	15.5569 ± 0.0897	—
$(a_p + a_s) \sin i$ / R	29.7536 ± 0.1789	29.70 ± 0.13
m_s / m_p	0.9126 ± 0.0110	0.915 ± 0.008

CONCLUSIONS

A Probabilistic Neural Network to derive the orbital elements of spectroscopic binary stars was applied. PNNs are used in both regression (including parameter estimation) and classification problems. However, one can discretize a continuous regression problem to such a degree that it can be represented as a classification problems[24,25], as we did in this work.

Using the measured V_R data of 66 And, HR 6979, HR 9059, Par 1802 and QX Car (HD 86118) obtained by Fekel et al.[5], Cargile et al.[3] and Andersen et al.[1], respectively, we find the orbital elements of these systems by the PNN. Our numerical results show that the results obtained for the orbital and spectroscopic parameters agree well with those obtained by others using traditional methods.

This method is applicable to orbits of all eccentricities and inclination angles. In this method the time consumed is considerably less than the method of Lehmann-Filhés. It is also more accurate as the orbital elements are deduced from all points of the velocity curve instead of four in the method of Lehmann-Filhés. The present method enables one to vary all of the unknown parameters γ, K, e and ω simultaneously instead of one or two of them at a time. It is possible to make adjustments in the elements before the final result is obtained. There are some cases, for which the geometrical methods are inapplicable, and in these cases the present one may be found useful. One such case would occur when observations are incomplete because certain phases could have not been observed. Another case in which this method is useful is that of a star attended by two dark companions with commensurable periods. In this case the resultant velocity curve may have several unequal maxima and the geometrical methods fail altogether.

REFERENCES

[1] J.Andersen, J.V.Clausen, B.Nordstrom, B.Reipurth; Absolute dimensions of eclipsing binaries, A&A, **121**, 271 **(1983)**.

[2] M.Bazarghan, H.Safari, D.E.Innes, E.Karami, S.K.Solanki; A nanoflare model for active region radiance: application of artificial neural networks, A&A, **492**, L13 **(2008)**.

[3] P.A.Cargile, K.G.Stassun, R.D.Mathieu; Discovery of PAR 1802 as a low-mass, pre- main-sequence eclipsing binary in the orion star- forming region, AJ, **674**, 329 **(2008)**.

[4] H.D.Curtis; Methods of determining the orbits of spectroscopic binaries, PASP, **20**, 133 **(1908)**.

[5] F.C.Fekel, J.Tomkin, M.H.Williamson; New precision orbits of bright double-lined spectroscopic binaries. IV. 66 Andromedae, HR 6979 and HR 9059, AJ, **139**, 1579 **(2010)**.

[6] Z.Han, C.A.Tout, P.P.Eggleton; Low and intermediate-mass close binary evolution and the initial - Final mass relation, MNRAS, **319**, 215 **(2000)**.

[7] K.Karami, R.Mohebi; Velocity curve analysis of spectroscopic binary stars AI Phe, GM Dra, HD 93917 and V502 Oph by nonlinear regression, ChJAA, **7**, 558 **(2007a)**.

[8] K.Karami, R.Mohebi; Velocity curve analysis of spectroscopic binary stars PV Pup, HD141929, EE Cet and V921 Her by nonlinear regression, JApA, **28**, 217 **(2007b)**.

[9] K.Karami, H.Teimoorinia; Velocity curve analysis of the spectroscopic binary stars by the non-linear least squares, Ap&SS, **311**, 435 **(2007)**.

[10] K.Karami, R.Mohebi, M.M.Soltanzadeh; Application of a new non-linear least squares velocity curve analysis technique for spectroscopic binary stars, Ap&SS, **318**, 69 **(2008)**.

[11] K.Karami, R.Mohebi; Velocity curve studies of spectroscopic binary stars V380 Cygni, V401 Cyg, V523 Cas, V373 Cas and V2388 Oph, JApA, **30**, 153 **(2009)**.

[12] W.F.King; Determination of the orbits of spectroscopic binaries, ApJ, **27**, 125 **(1908)**.

[13] R.Lehmann-Filhés; Ueber Die Bestimung Einer Doppelsternbahn Aus Spectroskopischen Messungen Der Im Visionsradius Liegenden Geschwindigkeits component, AN, **136**, 17 **(1894)**.

[14] L.B.Lucy, M.A.Sweeney; Spectroscopic binaries with circular orbits, AJ, **76**, 544 **(1971)**.

[15] E.Parzen; On estimation of a probability density function and mode, annals of mathematical statistics, **33**, 1065 **(1962)**.

[16] R.M.Petrie; Astronomical Techniques, W.A.Hiltner, (Ed); University of Chicago Press, Chicago, **(1960)**.

[17] H.C.Plummer; Notes on the determinations of the orbits of spectroscopic binaries, ApJ, **28**, 212 **(1908)**.

[18] H.N.Russell; An improved method of calculating the orbit of a spectroscopic binary, ApJ, **15**, 252 **(1902)**.

[19] H.N.Russell; A short method for determining the orbit of a spectroscopic binary, ApJ, **40**, 282 **(1914)**.

[20] F.Schlesinger; The Algol-variable ä Librae, PALLO, **1**, 123 **(1910)**.

[21] M.Singh; The determination of a spectroscopic binary orbit, Ap&SS, **100**, 13 **(1984)**.

[22] J.Skuljan, D.J.Ramm, J.B.Hearnshaw; Accurate orbital parameters for the bright southern spectroscopic binary æ Trianguli Australis an interesting case of a near-circular orbit, MNRAS, **352**, 975 **(2004)**.

[23] W.M.Smart; Textbook on spherical astronomy, Sixth Edition, Cambridge University Press, Cambridge, 360 **(1990)**.

[24] D.F.Specht; In Proceedings of the IEEE International Conference on Neural Networks, Calif. 2427, San Diego, 525 **(1988)**.

[25] D.F.Specht; Probabilistic neural networks. Neural Networks, **3**, 109 **(1990)**.

[26] T.E.Sterne; Notes on binary stars. V. The determination by least-squares of the elements of spectroscopic binaries, PNAS, **27**, 175 **(1941)**.

[27] K.Yakut, P.P.Eggleton; Evolution of close binary systems, ApJ, **629**, 1055 **(2005)**.